Self-broadening and exciton line shifts in gases: Beyond the local-field approximation

Jan A. Leegwater and Shaul Mukamel
Department of Chemistry, University of Rochester, Rochester, New York 14627
(Received 11 February 1993)

The dielectric function and the absorption line shape of a gas of polarizable atoms are calculated using numerical simulations and analytical approximations. The theory of self-broadening is recast in the framework of disordered excitons. The shift, width, and asymmetry of the absorption line shape are calculated and compared with recent experiments on potassium gas.

PACS number(s): 32.70.Jz

I. INTRODUCTION

A universal concept in the physics of line spectra of gases is that only two atoms need to be considered at low pressures. Properties of the gas phase then follow as a suitable cumulant expansion. This notion is so pervasive that it is usually taken for granted. The spectral shift and broadening are calculated using the two-particle approximation [1–5] both in the fast-collision (impact) limit as well as in the opposite, static limit. While for a gas in which the optically active atoms are perturbed by foreign atoms this can be justified, we will show that this no longer is the case for self-broadening, where at any density many-particle effects have to be taken into account.

Spectral line shapes are most conveniently classified as either homogeneous or inhomogeneous. A line is considered to be homogeneously broadened when the dominant broadening mechanism is due to the nuclear motions of the atoms (collisional broadening), and inhomogeneous if the broadening is mainly caused by a distribution of transition frequencies (the static line shape) [6] which for our model holds for particles with infinite mass. These names refer to the line shape in the vicinity of the center. Foreign-atom broadening in the gas phase is usually homogeneous. It has then been natural for researchers approaching the problem of self-broadening from the foreign-atom-broadening end [1] to ignore inhomogeneous broadening for self-broadening as well.

The problem of spectral line shapes of mixed crystals is based on the opposite view (the static limit); nuclear motions are totally neglected and the line shape is treated as inhomogeneous [7–9]. In these treatments the importance of having both attractive and repulsive interactions leading to both a blue and a red wing is usually not addressed. Consequently, the spectrum of a collection of polarizable atoms at finite (though low) density is usually addressed in the gas phase with the neglect of inhomogeneous contributions and in the solid state with the neglect of homogeneous contributions.

The experimental distinction between homogeneous and inhomogeneous broadening can be made in several ways. In the realm of linear optics we may either rely on a different line shape (e.g., a homogeneous Lorentzian profile and an inhomogeneous Gaussian profile) or use some argument that by varying a certain variable, such as temperature or density, one of the mechanisms may become dominant. As an example, the Doppler inhomogeneous profile has a width proportional to $(k_B T)^{1/2}$. One peculiar and important point that emerges out of the present study is that it is impossible to make this distinction for self-broadened resonance lines in the gas phase. Both mechanisms give a Lorentzian-like line profile and, moreover, the static and collision widths are of comparable magnitude, with a fixed ratio of 8:3, respectively, regardless of density or temperature. This implies that both broadening mechanisms must be treated simultaneously using a unified approach. The systematic investigation of both contributions in the same theory is one of the goals of the present article.

The only direct and unambiguous way of probing the nature of the line shape and its homogeneous or inhomogeneous character is provided by nonlinear optical methods such as photon echoes and hole burning [10]. A theory of these phenomena for interacting atoms at finite density still remains to be developed [8,9,11].

In Sec. II we present the Hamiltonian and introduce the formal definition of the frequency and wave-vector-dependent dielectric function $\epsilon(k,\omega)$. In Sec. III we separate the long-range contributions to the dielectric function using the Clausius-Mosotti local-field approach. In Sec. IV we present numerical simulations of the dielectric function, the polarizability, and the density of states, and provide a simple interpretation of the simulation results in the wings. Moments of the line shape are discussed in Sec. V. Collisional broadening is incorporated in Sec. VI followed by a comparison with recent experiments in potassium gas. Finally, in Sec. VII we make a few comments on the applicability of these ideas to restricted geometries (nanostructures) focusing on a two-dimensional quantum-well configuration.

II. THE HAMILTONIAN

Our model consists of a gas of polarizable atoms at low but finite density. Each atom is modeled as a four-level system representing a ground s state and a triply degenerate excited p state. We hereafter denote this the s-p model. We assume the following Hamiltonian:

$$H = H_D + H_{\text{nucl}} + H_{\text{int}} \ . \tag{1}$$

H_D is the electronic (dipole-dipole) part of the Hamiltonian

$$H_D=\hbar\sum_{n,i}\Omega B_{ni}^{\dagger}B_{ni}$$

$$+\hbar\sum_{\substack{n,m,i,j\\ n<m}}J_{ni,mj}(r_{nm})(B_{ni}^{\dagger}B_{mj}+B_{mj}^{\dagger}B_{ni})\ . \tag{2}$$

In the summation, n runs over the atoms, and i and j run over the internal degrees of freedom, $i,j=x,y,z$. All the atoms have the same isolated atom transition energies Ω. $B^{\dagger}$ and B are creation and annihilation operators for excitations of the s-p system at site n. As long as we restrict ourselves to linear optical properties, these can be considered to have the standard Bose commutation relations

$$[B_{nj},B_{mj}^{\dagger}]=\delta_{nm}\delta_{ij}\ . \tag{3}$$

The coupling J describes the dipole-dipole interaction between the atoms

$$J_{ni,mj}(r_{nm})=-\mu^2\left[\frac{3r_{nm,i}r_{nm,j}}{r_{nm}^5}-\delta_{i,j}\frac{1}{r_{nm}^3}\right](1-\delta_{n,m})\ , \tag{4}$$

with δ the Kronecker delta, $r_{nm}=r_n-r_m$, with r_n the position of atom n, and μ is the transition dipole moment that determines the magnitude of the dipole-dipole interaction. It can be related to the static polarizability α_0 by $\mu^2=\alpha_0\Omega/2$. The dipole-dipole interaction given here conserves the number of excitons (the Heitler-London approximation) [12]. It neglects terms of the form $B^{\dagger}B^{\dagger}$ and BB whose contributions are of order μ^2/Ω smaller than the terms considered, and can be safely neglected.

$H_{\rm nucl}$ is the Hamiltonian of the nuclear degrees of freedom

$$H_{\rm nucl}=\sum_n\frac{p_n^2}{2m_n}+\sum_{\substack{n,m\\ n<m}}V(r_{nm})\ , \tag{5}$$

and V represents the short-range internuclear interactions other than the dipole-dipole forces which are included in H_D. Van der Waals forces should be included in V as well since by invoking the Heitler-London approximation we have excluded them from the dipole part of the Hamiltonian. $V(r)$ is important in determining the equilibrium properties at elevated densities, and for the spectroscopy in the far wing [13]. In this paper we restrict ourselves to the vicinity of the line center and to gas-phase densities, and we put $V(r)=0$. Finally, $H_{\rm int}$ represents the interaction of the system with the external electric field,

$$H_{\rm int}=-\sum_{n,i}P_{ni}E_{ni}\ , \tag{6}$$

with the polarization operator

$$P_{ni}=\mu_n(B_{ni}^{\dagger}+B_{ni})\ . \tag{7}$$

Our goal is to calculate the dielectric function

$$\epsilon(k,\omega)=1+4\pi\chi^{(1)}(k,\omega)\ , \tag{8}$$

with the linear susceptibility tensor

$$\chi_{ij}^{(1)}(k,\omega)=\int_0^{\infty}dt\,\langle[P_{k,i}(0),P_{k,j}(t)]\rangle e^{i\omega t}\ , \tag{9}$$

where

$$P_{k,i}=\frac{1}{\sqrt{N}}\sum_n P_{ni}e^{ik\cdot r_n}\ . \tag{10}$$

Hence, the time evolution of P in the Heisenberg picture is

$$P(t)=\exp(iH_0t)P\exp(-iH_0t)\ , \tag{11}$$

with $H_0\equiv H_D+H_{\rm nucl}$.

When applied to a realistic system such as an alkali-metal gas we should add spin-orbit coupling to our present model. Our results are therefore expected to give a weighed average of properties of the two D lines of alkali-metal gases. The present theory may be applied to the spectrum of laser cooled atoms [14]. Extension of the results of optical nonlinearities will require using the Pauli rather than the Bose commutation rules [Eq. (3)] and constitute a complex and open challenge which will not be considered here [11,15].

There are four length scales in the problem that need to be considered in the analysis of the optical response. (i) The optical wavelength. We consider densities that are sufficiently high (many atoms in a volume of the wavelength cubed) that the wavelength can be considered infinite. (ii) The core radius of the atoms. As discussed before, we consider low densities and intermediate detunings so the core radius is not important. (iii) The Weisskopf radius, which is the radius for which a particle with thermal velocity has a collision phase shift 1. This radius is associated with the average cross section for collisional line broadening. (iv) The average interparticle distance. The average distance of an atom to its first nearest neighbor is

$$\bar{r}=\int d\mathbf{r}\,re^{-(4\pi/3)nr^3}$$

$$=\left[\frac{4\pi n}{3}\right]^{-1/3}\Gamma\left[\tfrac{4}{3}\right]\simeq 0.554n^{-1/3}\ , \tag{12}$$

where $n=N/V$ is the particle number density. An important feature of dipole-dipole interaction is that the nearest-neighbor distance determines the energy scale, a typical energy is $\bar{E}\equiv\mu^2/\bar{r}^3$. In fact, $\bar{E}$ is the *only* quantity determining the energy scale.

We shall hereafter consider gas-phase densities for which the nearest-neighbor distance is considerably smaller than the optical wavelength, yet larger than the range of the core potential as well as the Weisskopf radius. Then we can rescale the average interparticle distance to unity for any density. As the interaction is proportional to r^{-3}, the theory is independent of density after this rescaling, and there is *no length scale left in the problem*. In particular, we cannot perform a density expansion, not even at low density as there is no parameter left to expand in. At higher density (e.g., liquid densities)

the problem is more complex and will be treated in a future publication [16].

III. LOCAL-FIELD EFFECTS AND THE STATIC LIMIT

We shall first neglect the effects of nuclear motions and consider the static limit of the model. In the coming sections we discuss the static line shape; we return to the effect of nuclear motion in Sec. VI.

To gain some insight let us examine a regular lattice of atoms. In this case the isolated atom line is shifted by an energy which is the Fourier transform of J. As optical wavelengths typically are much larger than the interparticle separation we consider the $k \to 0$ limit. We have

$$J(k)=E_0(3\hat{\mathbf{k}}\hat{\mathbf{k}}-1) \tag{13}$$

with energy

$$E_0=\frac{4\pi}{3}n\mu^2=\frac{2\pi}{3}n\alpha_0\Omega \ . \tag{14}$$

The collective many-atom states (elementary excitations) for a lattice are called Frenkel excitons [12]. The longitudinal (transverse) excitons have a blueshift (redshift) of $2E_0$ (E_0). Only the transverse excitons are spectroscopically active, since electromagnetic waves are transverse. In the following we express energies in units of E_0.

For a disordered system one expects an analogue of this shift, however its calculation meets some formidable difficulties. For short-range interactions (decaying faster than r^{-3}) the relevant internuclear separations which contribute to the dipole correlation function are much shorter than the optical wavelength and we can safely make the long-wavelength ($k \to 0$) limit in our expressions. However, the dipole-dipole interactions are long range and contain a finite contribution of very far atoms separated by a distance larger than the optical wavelength. For this contribution the finite wavelength of light (finite k) needs to be carefully kept. A signature of this difficulty is that the expectation value of the potential energy $J(r)$ is only conditionally convergent.

Fortunately it is possible use a procedure due to Ewald [17] to separate the long-range and short-range contributions. To derive these results we partition the dipole-dipole interaction as follows:

$$J(r)=J_s(r)+J_l(r) \ , \tag{15}$$

where the J_s is of short range

$$J_s(r)=J(r)\exp(-r/R) \ , \tag{16}$$

and the long-range part is given by J_l,

$$J_l(r)=J(r)[1-\exp(-r/R)] \ . \tag{17}$$

Here, R is a cutoff distance. The idea is now to take R much larger than any correlation length in the problem, so that the contribution of J_l can be described using a local-field approximation.

For an infinite cubic lattice, the short-range dipole-dipole interaction does not produce the exciton line shift mentioned below Eq. (14); actually, it predicts no shift at all, and the exciton shift is due to the contributions of far-away atoms. Since the long-range contribution involves many atoms, fluctuations in the field they create on a particular atom (i.e., the local field) are negligible, and can be treated by a mean-field approximation which gives the Lorentz form for the local field $E_L=E+4\pi/P/3$. The resulting procedure is to use the short-range interaction to calculate α_s and substitute the final result in Clausius-Mosotti equation [18]

$$\frac{\epsilon(\omega)-1}{\epsilon(\omega)+2}=\frac{4\pi}{3}n\alpha_s(\omega) \tag{18}$$

with $\epsilon(\omega)$ being the $k \to 0$ limit of $\epsilon(k,\omega)$, which is the experimentally interesting quantity. The limit of $R \to \infty$ should be taken. α_{ij} represents the polarizability per atom. It is easy to show that for a Lorentzian α_s the Clausius-Mosotti equation produces a Lorentzian for ϵ which is shifted. We need to find

$$\alpha_{s,ij}(\omega)=\int_0^\infty dt\alpha_{s,ij}(t)e^{i\omega t} \ , \tag{19}$$

where

$$\alpha_{s,ij}(t)=\langle[P_{0,i}(0),P_{0,j}(t)]\rangle_s \tag{20}$$

is the short-range polarizability. $P(t)$ in Eq. (20) is calculated via Eq. (11) with a modified H_0 in which J is replaced by the short-range interaction J_s. While in principle this still depends on R, it should converge for $R \to \infty$.

The exact calculation of the dielectric function in the static limit for a system of N atoms requires the diagonalization of an $3N \times 3N$ matrix. Since the random matrix elements have diverging moments, the conventional theory of random matrices [19] does not apply to this case. In principle, N has to be very large, so that the box size has a volume larger than R^3. Introducing a basis set of exciton states

$$|k\gamma\rangle=N^{-1/2}\sum_n \exp(ik\cdot r)|n\gamma\rangle \ , \tag{21}$$

the static (no nuclear motions) polarizability is given by

$$\alpha_s(\omega)=\frac{\mu^2}{3\pi}\sum_{\gamma=x,y,z}\left\{\left\langle k=0,\gamma\left|\frac{1}{\omega-\Omega-\hat{J}_s+i0^+}\right|k=0,\gamma\right\rangle-\left\langle k=0,\gamma\left|\frac{1}{\omega+\Omega+\hat{J}_s-i0^+}\right|k=0,\gamma\right\rangle\right\} \ , \tag{22}$$

where $\hat{J}_s$ is the matrix whose elements are $J_{ni,mj}$ for a certain realization of particles, and the overbar denotes average over all positions, for any quantity A

$$\overline{A}=\frac{1}{V^N}\int dr_1 \cdots \int dr_N A \ . \tag{23}$$

Another important quantity that can be calculated using the same matrix is the density of states

$$\rho_D(\omega)=\frac{1}{3\pi N}\mathrm{Im}\sum_{k,\gamma=x,y,z}\overline{\left\langle k,\gamma\left|\frac{1}{\omega-\Omega-\hat{J}_s-i0^+}\right|k,\gamma\right\rangle} \ . \tag{24}$$

We shall calculate it as well, and use it in the analysis of the dielectric function.

A few comments are now in place. The Clausius-Mosotti equation results in a spectral shift and no broadening. This is natural since in its derivation we have neglected the effects of fluctuations in the long-range contributions. To illustrate this consider a Lorentzian form of the polarizability

$$\alpha(\omega)=2\mu^2\frac{\Omega+i\Gamma}{\omega^2-(\Omega+i\Gamma)^2} \ . \tag{25}$$

When this is substituted in Eq. (18) we get

$$\epsilon(\omega)=1+\frac{4\mu^2 n}{3}2\frac{\Omega'+i\Gamma}{\omega^2-(\Omega'+i\Gamma)^2} \tag{26}$$

with $\Omega'\equiv\Omega-E_0$. In this case $\epsilon(\omega)$ is also a Lorentzian, redshifted by E_0. The invariance of the line shape under the local-field correction is a special property of the Lorentzian form. For other line shapes local-field effects will also alter the shape itself. The fact that the averaging over the inhomogeneous distribution in Eq. (22) is performed on α and not on ϵ also reflects the short-range nature of the relevant inhomogeneous fluctuations and the neglect of fluctuations in the local field.

IV. SIMULATION RESULTS AND THEIR INTERPRETATION

We have simulated the polarizability in the static limit. While we called J_s a short-range interaction, it is still very long range compared to box sizes attainable in simulations. We therefore treated it using periodic boundary conditions. The limit $R\to\infty$ can then be taken, using the Ewald summation, replacing the dipole-dipole interaction by an effective one [20],

$$J_{ij}^{(eff)}(r)\equiv\lim_{R\to\infty}\sum_{r'}\exp\left[-\frac{r+r'}{R}\right]J_{i,j}(r+r') \ , \tag{27}$$

where r' runs over the simple cubic direct lattice. This limit can be taken analytically, resulting in a rapidly converging series expression for $J^{(eff)}$ [20]. In this approximation the large distance contribution of the dipole-dipole interaction is partially taken into account, and the remaining large distance effects are taken care of by the Clausius-Mosotti formula. By imposing periodic boundary conditions we make the system into a lattice with many particles in a unit cell. In this language what we have calculated corresponds to the zero wave-vector Frenkel exciton Bloch functions.

The simulation was done by putting $N=256$ particles at random positions. The density of states and polarizability were calculated by numerically diagonalizing the matrix $J_{ni,mj}^{(eff)}$ and averaging the results over 500 configurations.

Since both the real and imaginary parts are of interest we have plotted them separately. We adopt the common notation

$$\alpha(\omega)=\alpha'(\omega)+i\alpha''(\omega) \ . \tag{28}$$

The resulting polarizability is displayed in Fig. 1. As is clearly demonstrated in the figure, the maximum of $\alpha''(\omega)$ is redshifted compared with the isolated atom. We shall denote this shift by Δ. It also has an asymmetric line shape with a large tail on the red side. We shall characterize it by its value at half-maximum to the blue (Γ_+) and to the red (Γ_-) side. We further introduce the shift to the width ratio

$$\eta\equiv\frac{\Delta}{\Gamma_++\Gamma_-} \tag{29}$$

and an asymmetry parameter

$$S\equiv\frac{\Gamma_--\Gamma_+}{\Gamma_++\Gamma_-} \ . \tag{30}$$

The values of these parameters are listed in Table I. By substituting the simulated polarizabilities in the Clausius-Mosotti equation (18) we have obtained the frequency-dependent dielectric function which is displayed in Fig. 2. As for α, we denote the real and imaginary parts of ϵ by

$$\epsilon(\omega)=\epsilon'(\omega)+i\epsilon''(\omega) \ . \tag{31}$$

The parameters characterizing the absorption line shape $\epsilon''(\omega)$ are listed in Table I as well.

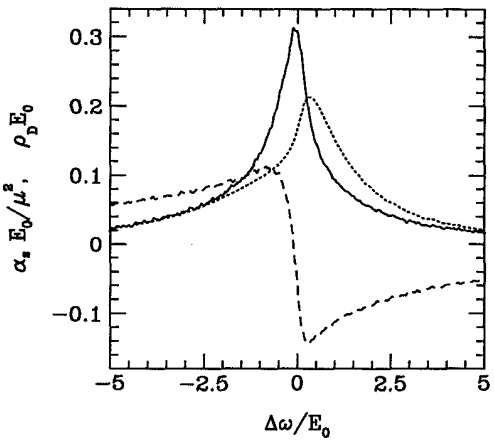

FIG. 1. Simulation results for the polarizability $\alpha_s(\omega)$. Solid line: the imaginary part $\alpha''(\omega)$; dashed line: the real part $\alpha'(\omega)$. Parameters describing α'' are given in Table I. The dotted line is the density of states.

TABLE I. The maximum Δ, width at positive half-maximum Γ_+, width at negative half-maximum Γ_- in units E_0. We also present the relative shift $\eta=\Delta/(\Gamma_++\Gamma_-)$ and asymmetry ratio $S=(\Gamma_--\Gamma_+)/(\Gamma_-+\Gamma_-)$.

Case	Δ	Γ_+	Γ_-	η	S
$\alpha^{(sim)}_{static}$	−0.09	0.54	0.92	−0.062	0.26
$\alpha^{(sim)}_{static+coll}$	−0.098	0.948	1.257	−0.044	0.14
$\alpha^{(anal)}_{static}$	−0.462	2.09	2.09	−0.11	0
$\alpha^{(anal)}_{static+coll}$	−0.462	2.88	2.88	−0.08	0
$\epsilon^{(sim)}_{static}$	−0.77	0.76	1.51	−0.40	0.40
$\epsilon^{(sim)}_{static+coll}$	−0.827	1.011	1.895	−0.285	0.304
$\epsilon^{(anal)}_{static}$	−1.462	2.09	2.09	−0.393	0
$\epsilon^{(anal)}_{static+coll}$	−1.462	2.88	2.88	−0.254	0
K $(S_{1/2}\leftrightarrow P_{1/2})$[a]				−0.28	
K $(S_{1/2}\leftrightarrow P_{3/2})$[a]				−0.285	

[a]Experimental results of Maki *et al.* [25].

Using the same simulation we have also calculated the density of states. The results are displayed in Fig. 1. Obviously, the density of states is very different from $\alpha''(\omega)$, contrary to what is usually assumed for static broadening in a gas [1].

To get a feeling for these results let us consider a system with only two atoms. In this case the six eigenfunctions are

$$|e_\pm\rangle=\frac{1}{\sqrt{2}}(|1i\rangle\pm|2i\rangle)\,, \tag{32}$$

with energies $\pm J_i$, $J_i=\mu^2 r_{12}^{-3}(-2,1,1)$, and $i=(x,y,z)$ where the x axis lies along $\mathbf{r}_{12}$. Only the three+states have a finite transition moment and are spectroscopically active. The eigenfunctions of the full N-particle problem are much more complex. Yet, Eq. (32) applies to situations where two atoms are very close, hence the energy involved is large compared to the interaction with third particles. Third particles mainly affect the line center and cause only small perturbations to the wings.

The traditional expression for the absorption at a sizable distance from resonance (line wings) is [21]

$$\alpha_2''(\omega)=\frac{n}{3}\sum_i\int d\mathbf{r}\,\delta(\omega-\Omega+J_i(\mathbf{r}))e^{-4\pi n r^3/3}\,. \tag{33}$$

We take only the spectroscopically active eigenvalues $+J_i$ here. The subscript 2 is to emphasize that this is a two-atom approximation.

The physical ingredients to Eq. (33) are, first, that the interactions are pairwise additive, the energy of a certain line is shifted from the isolated atom transition frequency Ω to $\Omega+J_i(r)$ by the perturbation. The large spectral shifts in the line wings primarily result from configurations with very short internuclear separations, which are rare events and can be assumed to occur one at a time. For the line core this approximation is harder to justify. Second, the exponential factor of Eq. (33) is supposed to correct for many particle effects by taking into account only the first neighbor. It represents the Poisson statistics of the nearest-neighbor distribution. For large distances we have no contribution.

$\alpha_2''(\omega)$, which is displayed in Fig. 3, demonstrates an

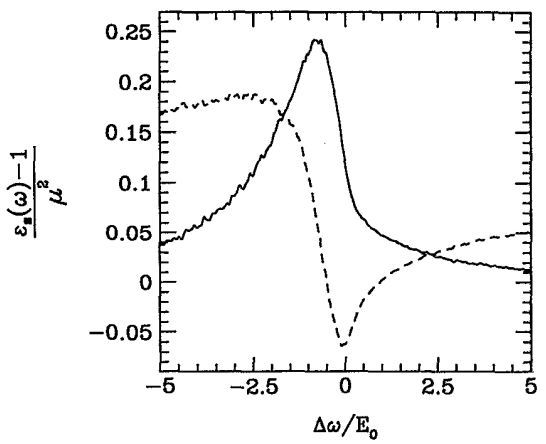

FIG. 2. Simulation results for the dielectric function $\epsilon(\omega)$. Solid line: The imaginary part of the static frequency-dependent dielectric function ϵ_s''; dashed line: the real part ϵ_s'.

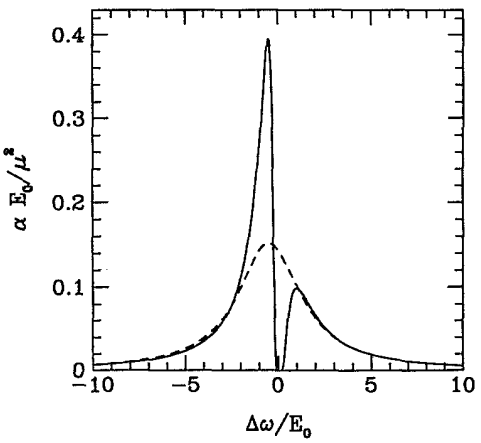

FIG. 3. Solid line: the imaginary part of the two-atom polarizability α_2'', Eq. (33). Even though for this absorption spectrum $\int_{-\infty}^{\infty}d\delta\omega\,\delta\omega\rho_0(\delta\omega)=0$, the spectrum appears asymmetric to the red (negative energy). The dashed line is a Lorentzian line with shift $\Delta_s=2\ln(2)E_0/3$, and width $\Gamma_s=(2\pi/3)E_0$, as calculated in Sec. IV.

important point; the origin of the redshift of $\alpha''(\omega)$. We can understand the distinction between the density of states and the absorption spectrum from the eigenfunctions Eq. (33). Instead of summing over just the $+J_i$ we also have to include the eigenvalues $-J_i$ for the density of states, so that to the same level of approximation

$$\rho_D(\omega)=\tfrac{1}{2}[\alpha_2''(\omega)+\alpha_2''(-\omega)] . \tag{34}$$

Obviously, $\rho_D(\omega)$ is symmetric.

However, as is apparent from Fig. 3, Eq. (33) is not a good approximation at all for the line core. There are third particles at larger distances and they will shift the resonance line some more, by (small) positive or negative random amounts. As there are many particles involved, the combined effect of all but the nearest neighbor is to contribute a random energy shift to the two particle line Eq. (33).

We next develop an approximate expression for the N-particle line shape. We consider the spectrum of two atoms in a box,

$$\alpha''(\Delta\omega)=\frac{n}{3}\sum_i \int d\mathbf{r}\,\delta(\Delta\omega+J_i(\mathbf{r})) . \tag{35}$$

Again, we sum only over $+J_i$ as these carry the dipole moment. It is easy to show that $\alpha''(\Delta\omega)\propto 1/\Delta\omega^2$ for a bounded range of $\Delta\omega(\Delta\omega\equiv\omega-\Omega)$. For small values of $\Delta\omega < A$, where $A=4\pi J/3V$ with V the volume of the box, Eq. (35) is no longer valid as then two particles are further away than the edge of the box (we assume a spherical box). At the high-energy end particles cannot be closer than a certain radius, say a hard-core radius σ. In terms of energy this translates to $B=J/\sigma^3$. The two-atom spectrum is then given by

$$\rho_2(\Delta\omega)=\tfrac{2}{3}\Theta(\Delta\omega)\rho_1(\Delta\omega)+\tfrac{1}{6}\Theta(-\Delta\omega)\rho_1(-\Delta\omega/2) , \tag{36}$$

where Θ is the unit step function and ρ_1 is given by

$$\rho_1(\Delta\omega)=C\frac{1}{(\Delta\omega)^2}\Theta(\Delta\omega-A)\Theta(B-\Delta\omega) . \tag{37}$$

C is a normalization constant.

We shall construct the full N-body spectrum out of ρ_2 by assuming that various perturbers are independent. For the N-atom spectrum we then only need to convolute ρ_2 N times with itself. At this step we use an assumption similar to that made in foreign-atom broadening, namely that the wave function for a perturbed system is close to the unperturbed system. As shown in the Appendix we find

$$\alpha_s(t)=\exp(-i\Delta_s t-\Gamma_s t) . \tag{38}$$

An exponentially decaying $\alpha_s(t)$ corresponds to a Lorentzian $\alpha_s(\omega)$. The resulting final spectrum is a Lorentzian with full width at half maximum (FWHM)

$$\Gamma_s=2\pi E_0/3 \tag{39}$$

and shift

$$\Delta_s=2\ln(2)E_0/3 . \tag{40}$$

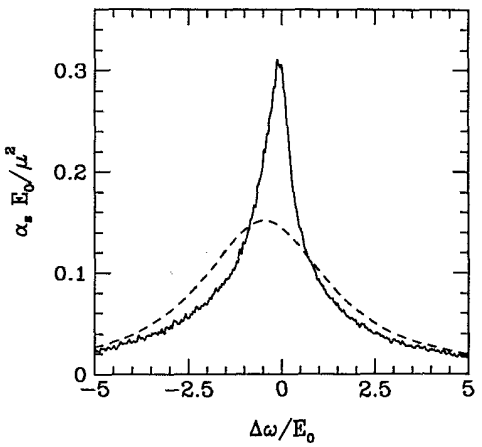

FIG. 4. Simulation results for the polarizability α_s'' (solid line). The dashed line is a Lorentzian with width $\Gamma_s=2\pi E_0/3$ and shift $\Delta_s=2E_0(\ln 2)/3$ [Eqs. (38)–(40)]. Only in the high-detuning wings the polarizability α_s is a Lorentzian.

Obviously, the resulting spectrum is only a Lorentzian after we take the limit $B\to\infty$. As our simulations have clearly shown large deviations from a Lorentzian, the assumption of independent perturbations cannot be justified. As shown in Fig. 4, the Lorentzian gives quite a good approximation in the wings but is crude at the center.

V. SUM RULES AND THEIR CONSEQUENCES

There is a sum rule valid for the exact N-particle spectrum,

$$\int_{-\infty}^{\infty} d\delta\omega\,\delta\omega\alpha''(\delta\omega)=\langle k=0|J^{(\mu)}|k=0\rangle=0 .$$

When considering the α'' integral this is not immediately obvious. It critically depends on the line wing behavior as the quantity integrated over is proportional to $1/\delta\omega$ hence the integral is conditionally convergent. To be more precise, we have

$$\int_{-\delta\omega_c}^{2\delta\omega_c} d\delta\omega\,\delta\omega\alpha''(\delta\omega)=0 , \tag{41}$$

where $\delta\omega_c$ is a large, arbitrary cutoff energy. This integral does not produce 0 for an unshifted Lorentzian and so is not a good measure of a possible shift. For the line core, a more appropriate description of an apparent shift is

$$\int_{-\delta\omega_c}^{\delta\omega_c} d\delta\omega\,\delta\omega\alpha''(\delta\omega)=-(2\ln 2/3)E_0 , \tag{42}$$

where we have used the fact that in the wings Eq. (37) is exact. *The center of the absorption spectrum is thus shifted to the red, though the first moment does not predict this shift.* This shows that the first moment is not a good measure of the spectral shift. This subtle point is often overlooked.

We note that the sum rule Eq. (42) immediately gives that the absorption is symmetric in the line wings. This agrees with experimental findings on the 1850-Å line of

mercury [22], but disagrees with experiments on cesium [23], where a factor of two difference between the absorption strength of the red and the blue wing at identical detuning was found. This intensity difference cannot be understood within the context of the present model. One possible explanation is that this is a consequence of spin-orbit coupling, which we have not taken into account.

If we fit the line obtained from Eq. (33) to a Lorentzian by matching the intensities in the far wings, we obtain for the width $2\pi E_0/3$, which equals the width calculated in Eq. (39).

Similar sum rules hold for the density of states ρ_D, where

$$\int_{-E_c}^{E_c} d\Delta\omega\, \rho_D(\Delta\omega)\Delta\omega = 0 , \tag{43}$$

as the two-particle density of states is symmetric. This proves that even at arbitrarily low densities, the absorption spectrum and the density of states differ.

VI. NUCLEAR MOTION AND COLLISIONAL BROADENING

So far all our calculations were made in the static limit where nuclear motions have been neglected. We shall now incorporate these motions in our theory. Collisional effects on self-broadening have been studied extensively in the past. Since there are discrepancies among the expressions reported in the literature [3,1] which differ by factors related to state degeneracy, we give a full derivation of the cross section.

We assume that the effect of collisions is independent of the static distribution. Then

$$\alpha(t) = \alpha_s(t)\alpha_{\rm coll}(t) . \tag{44}$$

However, in contrast to what has been implicitly assumed in previous calculations [2], it is not possible to neglect one of these factors since both of them decay on a comparable time scale.

Collisions produce a simple exponential decay for $\alpha(t)$,

$$\alpha_{\rm coll}(t) = \exp(-\Gamma_c t - i\Delta_c t) . \tag{45}$$

The standard expression for the collisional linewidth Γ_c and shift Δ_c is [2]

$$\Gamma_c + i\Delta_c = n\tfrac{1}{3}{\rm tr}\int dv\, vf(v)\int db\, 2\pi b(1-S_{1,1}) , \tag{46}$$

where $S_{1,1}$ are the 3×3 scattering matrix elements for a collision characterized by the impact parameter $\mathbf{b}$ and velocity $\mathbf{v}$. We have $S = \mathcal{O}_t \exp[i\int_{-\infty}^{\infty} dt\, J_{1i,2j}(t)]$ where $J_{1i,2j}$ is a 6×6 matrix. Though $J(t_1)$ does not commute with $J(t_2)$ the time ordering can be interchanged in a first approximation. Due to the properties of the trace, this is exact to second order in the interaction J.

In this semiclassical approximation we obtain

$$S_{ij} = (e^{i\Phi})_{1i,1j} \tag{47}$$

with [using Eq. (32)]

$$\Phi_{ni,mj} = \frac{1}{\hbar}\int_{-\infty}^{\infty} dt\, J(t) = |e_+\rangle\Phi_{ij}\langle e_+| - |e_-\rangle\Phi_{ij}\langle e_-| \tag{48}$$

$$\Phi_{ij} = \frac{J}{\hbar}\frac{2}{vb^2}(\delta_{i,j} - 2\hat{\mathbf{b}}_i\hat{\mathbf{b}}_j - \hat{\mathbf{v}}_i\hat{\mathbf{v}}_j) \tag{49}$$

where a $\hat{\mathbf{b}}$ denotes the unit vector in the direction of $\mathbf{b}$. Φ_{ij} has the eigenvalues $2J/\hbar vb^2(1,0,-1)$. Taking the $(1,1)$ matrix element of the S matrix and working out the trace we obtain a shift that is zero and a collision width

$$\Gamma_c = \frac{2\pi}{3} n\,{\rm tr}\int dv\, vf(v)\int db\, b\left[1-\cos\left[\frac{2\mu^2}{\hbar vb^2}\right]\right] = \frac{4\pi}{3}\frac{\mu^2}{\hbar} n\int_0^{\infty} dx\, x(1-\cos x^{-2}) . \tag{50}$$

Calculating the last integral we find the collision width and shift

$$\Gamma_c = \frac{\pi}{4}E_0 , \qquad \Delta_c = 0 . \tag{51}$$

Collision self-broadening is usually interpreted in terms of a cross section $\sigma_c = \pi b_0^2$, b_0 being the Weisskopf radius, defined as the impact parameter for which a particle with thermal velocity has a phase shift 1. Setting $\Gamma_c = n\sigma_c v_{\rm th}$ we get

$$b_0 = \left[\frac{2\mu^2}{v_{\rm th}}\right]^{1/2} , \tag{52}$$

where the thermal velocity is $v_{\rm th} = (k_B T/m)^{1/2}$, with k_B the Boltzmann constant, T the temperature, and m the mass of the particles.

Collisional broadening does not depend on the temperature or the mass, which is quite remarkable. Even more remarkable is that it is proportional to the Lorentz shift E_0, which is completely of static origin. We find that there is no small parameter to expand in, and a separation of the broadening process into "static" and "dynamic" contributions is somewhat artificial.

At this point we can add the collisional contribution via Eq. (44) to our previous calculation of the static polarizability α_s. Our most rigorous result will be to combine it with the simulations. The resulting α and ϵ are given in Fig. 5 and the relevant parameters describing these lines are tabulated in Table I. In Fig. 6, which may be regarded as the most rigorous result of this paper, we compare α'' and ϵ'' to demonstrate the importance of local-field effects.

If we use the analytical expression for α_s [Eq. (38)] we obtain a more crude approximation

$$\alpha(\omega) = 2\mu^2\frac{\Omega+\Delta_s+i\Gamma}{\omega^2-[\Omega+\Delta_s+i\Gamma]^2} \tag{53}$$

and

$$\epsilon(\omega) = 1+\frac{4\mu^2 n}{3}2\frac{\Omega+\Delta+i\Gamma}{\omega^2-(\Omega+\Delta+i\Gamma)^2} \tag{54}$$

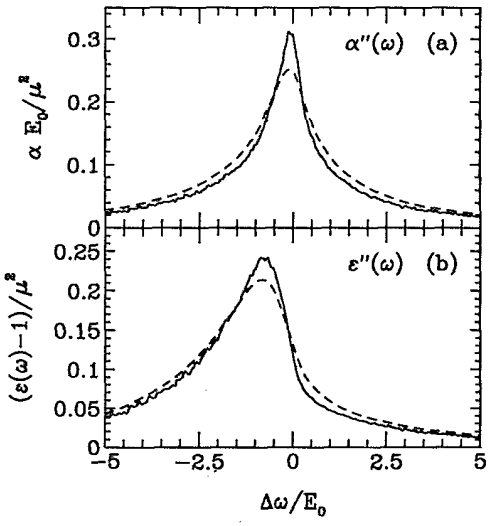

FIG. 5. Comparison of the simulated absorption without collisional broadening (solid line) and with collisional broadening (dashed). (a) The polarizability Eq. (44); (b) the dielectric function.

with a width that is a combination of static and collision widths

$$\Gamma=\Gamma_s+\Gamma_c=\left[\frac{2\pi}{3}+\frac{\pi}{4}\right]E_0=\frac{11\pi}{12}E_0\ , \tag{55}$$

and a shift which is the combination of the Lorentz shift and a new, static shift

$$\Delta=\Delta_s+E_0=(1+\tfrac{2}{3}\ln 2)E_0\ . \tag{56}$$

These parameters are listed in Table I as well for comparison with the simulation results. Previous calculations [3,1] have not taken into account the $[2\ln(2)/3]E_0$ shift, but predicted a collision width of $3E_0$, which is very close to our result and to experimental results.

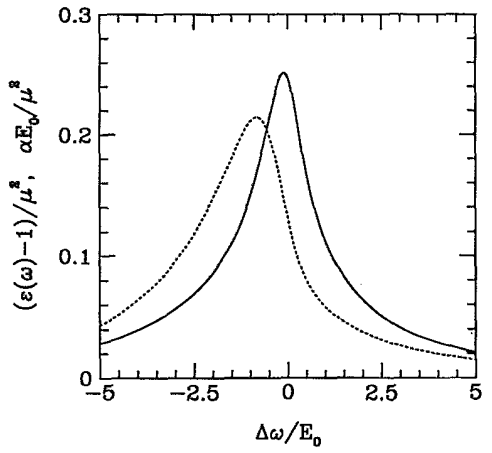

FIG. 6. Simulation results for the polarizability α'' (solid line) and ϵ'' (dotted line) where we included the collisional broadening [Eq. (44)].

The absorption of potassium gas in the density range 5×10^{15}–10^{17} $(\mathrm{cm})^{-3}$ has recently been studied [24,25] using selective reflection from a vapor. The reported shift-to-width ratio, which is almost identical for the two D lines, $\eta=0.28$. We find $\eta=0.285$ in our simulation and $\eta=0.254$ from our analytical theory (see Table I).

We shall now discuss additional effects that may possibly be of relevance. First of all we have neglected fine-structure splitting throughout. Our results are therefore expected to give a weighed average of properties of the two D lines of alkali-metal gases, while high-resolution experiments resolve the individual lines. We next consider the issue of length scales. The local-field shift is caused by the interaction with many atoms that are about an optical wavelength away. For a selective reflection experiment [26] as performed by Maki *et al.*, [24,25] it is well known that the electric field penetrates the gas a distance that is of the order of one wavelength [25], so *for selective reflection the local field is not fully developed.* In particular the shift of the absorption line depends on the position in the medium. It appears that this effect will cause an additional broadening and a decreased line shift. A rigorous calculation must solve in full detail the local field; α is a meaningful microscopic quantity, ϵ is less so as either it is not the macroscopic ϵ when we are near the surface, or it is experimentally inaccessible when it is inside the medium. The introduction of polaritons [15] is needed to describe the propagation properties inside the medium.

Another point is related to higher density effects. The relevance of the nearest-neighbor distances was discussed in the previous sections. Deviations from the dipole-dipole interaction are of relevance for high density. This has two consequences for the spectrum. (i) The random shifts become different, and (ii) the equilibrium properties of the fluid have to be calculated, making the spectrum a problem in liquid state theory. This is only important at very high density.

There is a question regarding the static and dynamic aspects of the problem. A unique property of the dipole-dipole interaction is that the static line gives a Lorentzian form in the tails, which is also the result of the dynamic theory. For one thing, this implies that the static and dynamic effects cannot be separated, and also that there is a density for which collisions are no longer completed before being interrupted by third particles. This occurs when the average interparticle distance is less than the Weisskopf radius. An estimate of the density at which this becomes important for Potassium at room temperature is 10^{18} cm^{-3}. This is the only quantity where the mass and temperature enter. For higher densities we expect the collisions to become even less important compared to static broadening. Additional effects neglected in our treatment are Van Der Waals forces as well as short-range deviations from the dipole-dipole interactions, i.e., contributions from higher multipoles. Both of these approximations are reasonable at low density.

VII. DIELECTRIC RESPONSE IN TWO DIMENSIONS

There is currently a great interest in confined systems in lower dimensionalities. It is now possible to fabricate

nanostructures where the atoms are confined to two dimensions [27]. For atoms physisorbed on surfaces at low concentration the calculations in two dimensions may also be of interest.

The long-range behavior of dipole sums, which is a very difficult problem in three dimensions (3D), is much less pathological in 2D and, consequently, the behavior is qualitatively different and the relative importance of the various scales mentioned earlier is quite different in two dimensions.

First, and most importantly, there is no need to introduce the local field, as the long-distance behavior of the dipole sums is convergent so rather than the Clausius-Mosotti equation (18), we now have,

$$\epsilon(\omega)=1+4\pi n\alpha(\omega)\ . \tag{57}$$

In addition, there is a difference in density dependence of the static and dynamic linewidth. Hereafter, we focus on the static contribution and neglect collision effects which are not important for a monolayer with fixed atomic positions.

The two-dimensional structures with the transition dipoles along the surface (for an aggregate this would be a J aggregate) are most similar to our three-dimensional calculations as the static shift can be both positive and negative. As an approximation we take the nearest neighbor fully into account, and convolute the resulting spectrum $\rho_0^{(2D)}$ by a Gaussian characterized by the average E_g and standard deviation w_g.

Explicitly, we have for the nearest neighbor,

$$\rho_0^{(2D)}(\Delta\omega)=\frac{2(\kappa E_2)^{2/3}}{3|\Delta\omega|^{5/3}}e^{-|\kappa E_2/\Delta\omega|^{5/3}} \tag{58}$$

with $E_2\equiv(n\pi)^{3/2}\mu^2$, $\kappa=1$ for $E>0$, and $\kappa=2$ for $E<0$.

The probability distribution of finding a particle other than the nearest neighbor at distance r is

$$n_2(r)=n(1-e^{-\pi nr^2})\ , \tag{59}$$

where N is the atom surface density. The expectation value of the energy is

$$\langle V(r)\rangle=E_g=-\sqrt{\pi}E_2\ . \tag{60}$$

The second moment $\langle[V(r)-E_g]^2\rangle$ diverges as well as $\langle|V(r)-E_g|\rangle$. To have some sort of measure of the width of the Gaussian we use the absolute value of $V(r)$,

$$\langle|V(r)|\rangle=3\sqrt{\pi}E_2$$
$$=\sqrt{(2/\pi)}w\exp\left[-\frac{E_g^2}{2w^2}\right]+|E_g|\mathrm{erf}\left[\frac{|E_g|}{w\sqrt{2}}\right]\ , \tag{61}$$

where erf is the error function. We find $w=4.806E_2$.

Combining these results we get

$$\alpha(\Delta\omega)=\mu^2\int\Delta\omega'\rho_0^{(2D)}(\Delta\omega-\Delta\omega')\Psi\left[\frac{\Delta\omega'-E_g}{w_g}\right]\ , \tag{62}$$

where Ψ is a Gaussian

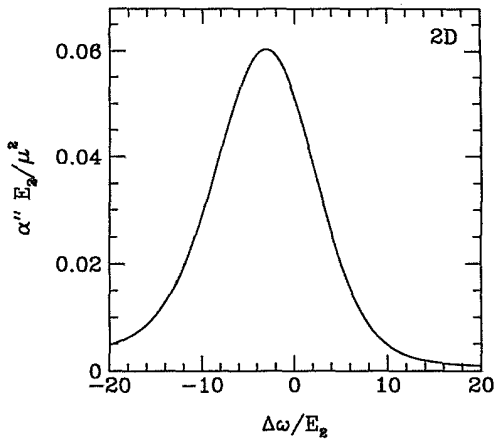

FIG. 7. The absorption spectrum in two dimensions, where the transition dipoles lie along the surface. We find a shift $\Delta=-3.07E_2$, widths $\Gamma_+=6.35E_2$, and $\Gamma_-=-6.7E_2$, so that the relative shift $\eta=-0.235$ and the asymmetry is $S=0.027$.

$$\Psi\left[\frac{\Delta\omega'-E_g}{w_g}\right]=(2\pi w_g^2)^{-1/2}\exp\left[-\frac{(\Delta\omega'-E_g)^2}{2w_g^2}\right]\ . \tag{63}$$

The resulting absorption spectrum is presented in Fig. 7.

ACKNOWLEDGMENTS

The support of the National Science Foundation and the Air Force Office of Scientific Research is gratefully acknowledged. We wish to thank Professor R. Boyd and Dr. J. Maki for useful discussions regarding their experiment.

APPENDIX: CALCULATION OF THE STATIC GAS-PHASE SPECTRAL SHIFT

In this appendix we derive Eq. (38). For technical reasons we use different cutoff factors as those used in ρ_1, $e^{-A/\Delta\omega}$ for large distances (small $\Delta\omega$), and $e^{-\Delta\omega/B}$ for short distances. We take the limit $B\to\infty$ in the end, since we are interested in the line center. These cutoff factors give instead of Eq. (37)

$$\rho_1(\Delta\omega)=C\frac{1}{(\Delta\omega)^2}\exp\left[-\frac{A}{\Delta\omega}-\frac{\Delta\omega}{B}\right]\Theta(\Delta\omega)\ . \tag{A1}$$

A practical way to perform the convolution mentioned in Sec. III is by means of Fourier transforms. The Fourier transform of ρ_2 is

$$F_2(t)=\int_{-\infty}^{\infty}d\Delta\omega\,\rho_2(\Delta\omega)e^{-i\Delta\omega t}$$
$$=\frac{2z_+K_1(z_+)+z_-K_1(z_-)}{3z_0K_1(z_0)}\ , \tag{A2}$$

where K_1 is a modified Bessel function [28], $z_+=2(iAt+A/B)^{1/2}$, $z_-=2(-2iAt+A/B)^{1/2}$, and $z_0=z_+(t=0)$. We have to the order in z that we need

$$zK_1(z)=1+\frac{z^2}{2}\left[\ln\frac{z}{2}+\gamma-\frac{1}{2}\right]+\cdots , \tag{A3}$$

where γ is Euler's gamma. Since the Fourier transform of the convolution is the product of the Fourier transforms, we finally obtain the Anderson-Talman expression [2]

$$\alpha_s(t)=F_N(t)=e^{\lambda(t)} \tag{A4}$$

with

$$\lambda(t)=N[F_2(t)-1]$$
$$=i\frac{2}{3}E_0(i\pi|t|+t\ln 2)+\mathcal{O}(1/B)+\mathcal{O}(A^2N) . \tag{A5}$$

As $A=E_0/N$ the limit $N\to\infty$ is well defined. Equations (A4) and (A5) are identical to Eq. (38).

[1] E. L. Lewis, Phys. Rep. **58**, 1 (1980).
[2] P. W. Anderson, Phys. Rev. **76**, 647 (1947); P. W. Anderson and J. D. Talman, Bell Telephone System Technical Publication No. 3117 (1956) (unpublished).
[3] A. W. Ali and H. R. Griem, Phys. Rev. **140**, 1044 (1965).
[4] A. Ben Reuven, Adv. Chem. Phys. **33**, 235 (1975).
[5] J. Szudy and W. E. Baylis, J. Quant. Spectrosc. Radiat. Transfer **15**, 641 (1975).
[6] E.g., V. S. Letokhov and V. P . Chebotayev, *Nonlinear Laser Spectroscopy* (Springer, Berlin, 1977).
[7] A. M. Stoneham, Rev. Mod. Phys. **41**, 82 (1969).
[8] C. A. Walsh, M. Berg, L. R. Narasinham, K. A. Littau, and M. D. Fayer, Chem. Phys. Lett. **134**, 268 (1986).
[9] F. C. Spano and W. S. Warren, J. Chem. Phys. **90**, 6034 (1989).
[10] Y. J. Yan and S. Mukamel, J. Chem. Phys. **94**, 179 (1991).
[11] J. A. Leegwater, L. Fried, and S. Mukamel, Z. Phys. D **26**, 126 (1993).
[12] A. S. Davydov, *Theory of Molecular Excitons* (Plenum, New York, 1971).
[13] R. E. M. Hedges, D. L. Drummond, and A. Gallagher, Phys. Rev. A **6**, 1519 (1972).
[14] J. Dalibard and C. Cohen-Tannoudji, J. Opt. Soc. Am. B **6**, 2125 (1989).
[15] J. Knoester and S. Mukamel, Phys. Rep. **205**, 1 (1991).
[16] J. A. Leegwater and S. Mukamel, J. Chem. Phys. **99**, 6062 (1993).
[17] M. Born and K. Huang, *Dyanmical Theory of Crystal Lattices* (Oxford, London, 1968).
[18] J. Knoester and S. Mukamel, Phys. Rev. A **39**, 1899 (1989); D. Bedeaux and N. Bloembergen, Physica **69**, 67 (1973); J. Van Kranendonk and J. E. Sipe, in *Progress in Optics,* edited by E. Wolf (North-Holland, Amsterdam, 1977), Vol. 15, p. 245; J. de Goede and P. Mazur, Physica **58**, 568 (1972); P. Madden and D. Kivelson, Adv. Chem. Phys. **56**, 467 (1984).
[19] M. L. Mehta, *Random Matrix Theory,* 2nd ed. (Academic, Boston, 1991).
[20] E.g., S. W. De Leeuw, J. W. Perram, and E. R. Smith, Proc. R. Soc. London Ser. A **373**, 27 (1980).
[21] H. G. Kuhn, Philos. Mag. **18**, 987 (1934); Proc. R. Soc. London Ser. A **158**, 212 (1937); H. Margenau, Phys. Rev. **48**, 755 (1935).
[22] D. Gebhard and W. Behmenburg, Z. Naturforsch. **30a**, 445 (1975).
[23] K. Niemax and G. Pichler, J. Phys. B **7**, 1204 (1974).
[24] J. J. Maki, M. S. Malcuit, J. E. Sipe, and R. W. Boyd, Phys. Rev. Lett. **67**, 972 (1991).
[25] J. J. Maki, Ph.D. Thesis, University of Rochester 1991 (unpublished).
[26] W. J. Condell and H. I. Mandelberg, J. Opt. Soc. Am. **54**, 973 (1964); J. P. Woerdman and M. F. H. Schuurmans, Opt. Commun. **14**, 248 (1975).
[27] F. F. So, S. R. Forrest, Y. Q. Shi, and W. H. Steiner, Appl. Phys. Lett. **56**, 674 (1990); F. F. So and S. R. Forrest, Phys. Rev. Lett. **66**, 2649 (1991).
[28] I. S. Gradshteyn and I. M. Ryzhik, *Table of Integrals, Series, and Products* (Academic, London, 1980).